Journal of Institute of Science and Technology, 31(1), 171-182 (2026)
ISSN: 2467-9062 (print), e-ISSN: 2467-9240
https://doi.org/10.3126/jist.v31i1.92566

Research Article

NICKEL-INCORPORATED CERIUM METAL ORGANIC FRAMEWORK ON NICKEL FOAM: UNVEILING 3D NANOPILLARS ON 3D SUBSTRATE FOR GREEN HYDROGEN GENERATION VIA WATER SPLITTING

Ishwor Pathak[1,2]*, Pujan Nepal[3], Keshav Raj Chapagain[2,4], Muna Niraula[5], Mani Ram Kandel[1], Prakash Chandra Lohani[1], Purna Prasad Dhakal[4], Bipeen Dahal[4], Tirtha Raj Acharya[2,6]*

[1] *Department of Chemistry, Amrit Campus, Tribhuvan University, Kathmandu, Nepal*
[2]*Advanced Nanomaterials & Green Energy Laboratory (ANGEL), Amrit Campus, Tribhuvan University, Kathmandu, Nepal*
[3] *Department of Chemistry, Jeonbuk National University, Jeonju, 54896, Republic of Korea*
[4] *Central Department of Chemistry, Tribhuvan University, Kathmandu, Nepal*
[5] *Ministry of Forest and Environment, Department of Forest and Soil Conservation, Babarmahal, Kathmandu, Nepal*
[6] *GSK Carbon Neutral Laboratories for Sustainable Chemistry, University of Nottingham, Jubilee Campus, Triumph Road, Nottingham NG7 2TU, UK*
**Correspondence: ishwor.pathak@ac.tu.edu.np,* tirtha.acharya@nottingham.ac.uk

(*Received*: April 4, 2026; *Final Revision*: May 10, 2026; *Accepted*: June 8, 2026)

ABSTRACT

For sustainable hydrogen production through water splitting, the rational engineering of economical and effective electrocatalysts/nanomaterials for the hydrogen evolution reaction (HER) is essential. In this work, we describe the logical design and in-situ development of a nickel-doped cerium metal-organic framework (Ni/Ce-BTC@NF) directly on 3D nickel foam (NF), designing a binder-free (freestanding) electrode with a distinctive three-dimensional (3D) nanopillar-like structure. The unique design of a crystalline Ce-BTC framework with evenly dispersed nickel while maintaining the intrinsic rod-like shape upon doping is confirmed by structural and morphological investigations. Electrochemical measurements reveal that Ni doping significantly enhances HER activity in alkaline medium, with Ni/Ce-BTC@NF achieving overpotentials of 108.9 mV and 196.1 mV to sustain 10 mA cm^{-2} and 50 mA cm^{-2}, respectively, outperforming pristine Ce-BTC@NF. Excellent durability is demonstrated by the material's steady activity throughout a 24-hour time of continuous operation. The Ni/Ce-BTC@NF (−) // RuO_2@NF (+) electrolysis configuration exhibits competitive total water-splitting performance requiring 1.67 V (cell voltage) at 10 mA cm^{-2}. This research offers a viable method for designing cerium MOFs-based electrocatalysts with hierarchical topologies and modulated electronic structures for effective hydrogen generation.

Keywords: Electrocatalyst, HER, MOFs, Water splitting

INTRODUCTION

Global reliance on fossil fuels for energy, together with the extensive pollution and ecological degradation resulting from their extraction and utilization, has created a worldwide necessity to swiftly advance sustainable renewable energy alternatives (Aryal et al., 2025; Pathak et al., 2025; Chhetri et al., 2026). Green hydrogen is considered as the fuel of the future due to its high energy efficiency, low cost, sustainability and ecological benign nature. A viable technique for producing hydrogen fuel, a clean and sustainable energy source, is electrochemical water splitting (Shetty et al., 2018; Zahra et al., 2020; Rosyara et al., 2025). This involves generation of hydrogen at the cathode ($2H_2O + 2e^- \rightarrow H_2 + 2OH^-$) and oxygen evolution reaction (OER) at the anode ($2H_2O \rightarrow O_2 + 4H^+ + 4e^-$) (Chhetri et al., 2022; Wang et al., 2023; Wu et al., 2023). To date, noble metals such as Pt and Ru/Ir have been extensively explored as benchmark electrocatalyst for HER and OER, respectively (Anantharaj et al., 2020; Pathak et al., 2025). Nevertheless, their limited availability, high price and poor durability constraint their potential commercialization in water splitting (Jamesh et al., 2019; Acharya et al., 2024; Pandey et al., 2026). Consequently, the fabrication of cost-effective, earth-abundant, and efficient

electrocatalysts has become a central focus in energy conversion research.

In this regards, noble-metal-free earth-abundant transition metal compounds such as transition metal dichalcogenides, selenides, phosphides, oxides, hydroxides, and carbides have been widely investigated as viable alternatives to precious metal catalysts (Amin et al., 2017; Yan et al., 2019; Amorim et al., 2020; Yu et al., 2020; Mondal et al., 2022; Rathore et al., 2022; Alkhaldi et al., 2024). In parallel, rare-earth (RE) elements have enticed attention in coordination chemistry due to their unique electronic configurations, high coordination numbers, and strong affinity toward O- and N-donor ligands, enabling the formation of structurally robust and chemically stable framework (Janicki et al., 2017; Jacobsen et al., 2020; Acharya et al., 2023). Among them, cerium is a promising low-cost candidate for stable MOF synthesis due to its high natural abundance comparable to common metals like copper, zinc, and tin, and significantly greater than other rare earth elements (Gu et al., 2024).

Metal-organic frameworks (MOFs), coordinated from metal nodes (mostly transition metals) and organic linkers, represent a class of unique crystalline porous materials that have acquired substantial attention in electrocatalysis due to their ample surface area, tunable composition, and well-defined active sites (Zhou et al., 2012; Naik Shreyanka et al., 2022; Pathak et al., 2024; Chhetri et al., 2025). Various MOF families, including zeolitic imidazolate frameworks, prussian blue analogues, carboxylate-based MOFs, and porphyrin-based MOFs, have demonstrated promising catalytic performances (Liu et al., 2021; Sirati et al., 2022). In this system, the abundant metal ions available at a fixed position or clusters and ample cavity in MOFs can act as catalytically active sites (Senthil et al., 2018; Senthil et al., 2019; Lu et al., 2020; Xie et al., 2020). Notably, Ce-based MOFs (Ce-MOFs) are of great interest due to their intrinsic redox activity, porous characteristics, low-energy 4f orbitals, and ability to generate oxygen vacancies, which can enhance catalysis by facilitating charge transfer kinetics. Moreover, the coexistence of Ce^{3+} and Ce^{4+} species can provide additional redox flexibility, further improving catalytic efficiency (Wu et al., 2018; Jacobsen et al., 2020; Hu et al., 2021). The study of Ce-MOFs has been dominated for many years by Ce(III)-MOFs, mainly including their synthesis and luminescent properties (Jacobsen et al., 2020; Hu et al., 2021). Furthermore, Ce(IV)-MOFs, whose chemistry has many similarities to that of Zr-MOFs, have attracted much scientific interest benefiting from their promising applications in redox catalysis and photocatalysis (Jin et al., 2021; Gu et al., 2022; Liu et al., 2022). In 2019, Jin et al. used a mixed valence Ce-MOF with isolated Ce(IV, III) redox couples and abundant oxygen vacancies as a separator coating material for the Li-S battery, which can effectively suppress the shuttle effect of polysulfides via accelerating their redox kinetics (Jin et al., 2021). Ce-MOFs are of special demand owing to synergy of 3D nanoarchitecture with ample surface area, the Ce(III)/(IV) redox behavior and the occurrence of low energy 4f orbitals. Thus, outstanding catalytic and luminescent properties are achievable (Jacobsen et al., 2020). Moreover, the structural and electrochemical characteristics of MOFs are significantly influenced by the choice of organic linker. In this regard, the tricarboxylate ligand, trimesic acid (1,3,5-benzenetricarboxylic acid, or simply BTC) is extensively used for constructing robust three-dimensional frameworks with diverse topologies, including sheets, chains, and interconnected networks. BTC-based MOFs exhibit excellent structural and electrochemical stability due to the presence of multiple coordination sites, making them highly suitable for catalytic applications (Wang et al., 2020).

Despite the aforementioned advantages, pure MOFs often suffer from poor electrical conductivity because of the insulating nature of organic ligands and limited overlap between metal d orbitals and ligand p orbitals. This inherent limitation restricts efficient effective transport during electrocatalysis (Zou et al., 2019; Wang et al., 2021; Pathak et al., 2023). More commonly, high-temperature carbonization has been employed to boost conductivity. However, it often leads to structural collapse, higher energy consumption, and loss of intrinsic MOFs properties (Xia et al., 2017; Rosyara et al., 2024). Therefore, alternative strategies that preserve the structural integrity while enhancing conductivity are highly desirable. Heteroatom doping is one of the effective approaches that can enhance catalytic activity and alter the electrical structure (Dong et al., 2020). In particular, cation doping induces charge imbalance within lattice, resulting the change in the surface charge distribution to regulate the adsorption energy of oxygen intermediates (Luo et al., 2023). In this context, nickel doping has been shown to significantly

enhance HER performance by reducing hydrogen adsorption free energy, facilitating water dissociation, and promoting intermediate desorption (Luo et al., 2019). Ni incorporation can induce lattice distortion and generate additional active sites, further improving catalytic efficiency (Dong et al., 2020). Furthermore, the synthesis of MOFs on porous and conductive 3D substrates enables to fabricate binder free freestanding electrode with improved mass transport, enhanced mechanical stability, and better exposure of active sites. Nevertheless, key challenges remain, including limited conductivity, insufficient active site accessibility, and weak interfacial integration with conductive supports. Addressing these issues requires rational design strategies involving compositional tuning and structural optimization.

In order to improve electrocatalytic water splitting, we present here a logical design and synthesis of Ni-doped Ce-based MOFs using BTC as an organic linker. It is anticipated that adding Ni to the Ce-MOFs framework will boost intrinsic catalytic activity, improve charge transfer, and modify the electronic structure. Moreover, using BTC as a linker guarantees structural stability and offers abundant coordination positions for effective catalysis. It is expected that enhanced electrocatalytic activity toward HER in alkaline conditions will result from the synergistic action between Ce and Ni as well as the structural benefits of BTC-based frameworks. The design of sophisticated MOFs-based electrocatalysts for sustainable hydrogen production is improved by this work.

MATERIALS AND METHODS

Materials (chemical and reagents)

Nickel foam, benzene-1,3,5-tricarboxylic acid (trimesic acid, 95%), cerium(III) nitrate hexahydrate (99%), platinum on carbon (10 wt.%), ruthenium(IV) oxide (99.9%), ethanol (99.5%), dimethylformamide (DMF, 99.5%), hydrochloric acid (35.0-37.0%), and acetone (99.7%) were purchased from Sigma-Aldrich.

Pretreatment of nickel foam (NF)

A piece of bare nickel foam (5 × 3 cm^2) was immersed in HCl (3 M) and sonicated for 20 min to eradicate surface impurities and oxide layer. The foam was then ultrasonically cleaned sequentially with acetone–distilled water–ethanol, and drying at 50 °C.

Preparation of nickel doped Ce-BTC MOF on nickel foam (Ce-BTC@NF)

Nickel nitrate hexahydrate (0.1 mmol), cerium nitrate hexahydrate (1 mmol), and benzene tricarboxylic acid (1.0 mmol) were dissolved in a mixed solvent of 20 mL DI water, 20 mL ethanol and 10 mL dimethylformamide (DMF). The resulting solvent mixture was stirred, then poured into a hydrothermal autoclave containing pre-cleaned nickel foam (NF), and treated at 120 °C for 2.5 h. The as-prepared material was removed after cooling, washed with ethanol and DI water, and oven dried (for overnight) to obtain Ni/Ce-BTC@NF. A similar procedure without the addition of nickel salt was used to prepare Ce-BTC@NF for comparison.

Material characterization

The crystal structure and phase purity of the samples were analyzed using X-ray diffraction (XRD, Rigaku, Japan) with Cu Kα radiation (λ = 1.5406 Å**)** operated at 40 kV over a 2θ range of 5–85°**.** The surface morphology was observed by field-emission scanning electron microscopy (FESEM), while energy-dispersive X-ray spectrometer (EDS) was used for elemental analysis**.**

Electrochemical characterization

Electrochemical measurements in two- and three-electrode set up were conducted in alkaline electrolyte (1 M KOH solution) at 25 °C. The as-prepared freestanding catalysts (1 × 1 cm^2) were used for working electrodes, while a Pt wire served as the counter electrode. Ag/AgCl was used in a position of reference electrode so that the three-electrode configuration was complete. For full cell electrolysis in two-electrode set-up, Ni/Ce-BTC@NF (1 × 1 cm^2) was employed as cathode and benchmark RuO_2@NF with identical size and mass loading (2.5 mg cm^{-2}) was employed as an anode. Linear sweep voltammetry (LSV) curves were scanned at 2 mV s^{-2} scan rate, and electrochemical impedance spectroscopy (EIS**)** test was carried out at 5 mV RMS amplitude and 0.01 Hz–100 kHz frequency. The stability test of the MOF-catalysts was assessed by chronoamperometry (CA) tests.

RESULTS AND DISCUSSION

Physicochemical analysis

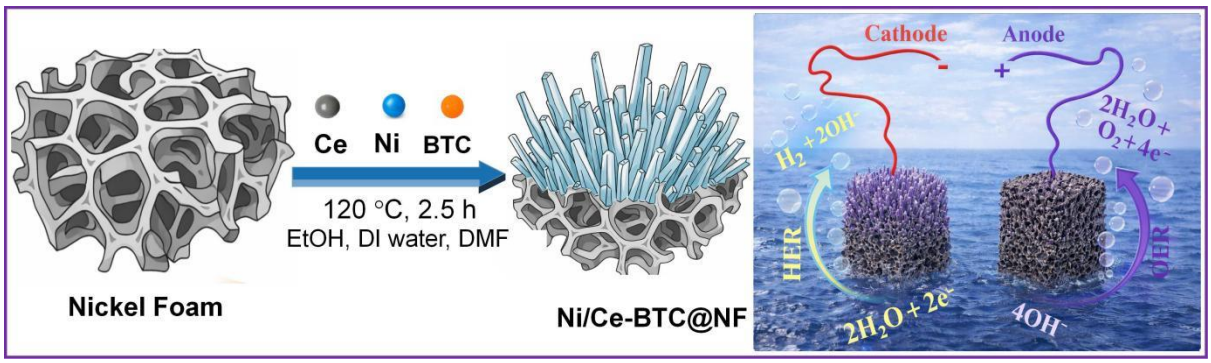

Scheme 1. Diagrammatic illustration for the preparation of Ni/Ce-BTC@NF and its application for HER

The XRD curve of the as-prepared Ni/Ce-BTC@NF is presented in Figure 1. The peaks that appeared at 2θ value of 8.4°, 10.6°, and 18.1° reveal that the obtained Ce-BTC is highly crystalline, which is consistent with previous reported results (Zhang et al., 2017, 2018). The additional intense reflections at 2θ = 44.5°, 51.8°, and 76.4° are indexed to metallic nickel (PDF #04-0850), originating from the nickel foam substrate as well as the nickel dopant. The morphological analysis of Ce-BTC@NF and Ni/Ce-BTC @NF were assessed through FESEM as depicted in Figure 2. The Ni-doped Ce-BTC@NF (Fig. 2a, 2b, 2c) exhibits a well-defined hierarchical microflower-like architecture composed of radially aligned rod-like subunits, forming an interconnected nanopillars like porous network. This structure provides a high surface area and facilitates efficient electrolyte diffusion and gas release during HER. Notably, the 3D rod-shaped Ce-BTC MOFs (Fig. 2d) remained unchanged after the Ni doping. The EDS elemental mapping images and spectrum (Fig. 3) show the homogenous distribution of the constituent elements in the cerium MOF nanorod.

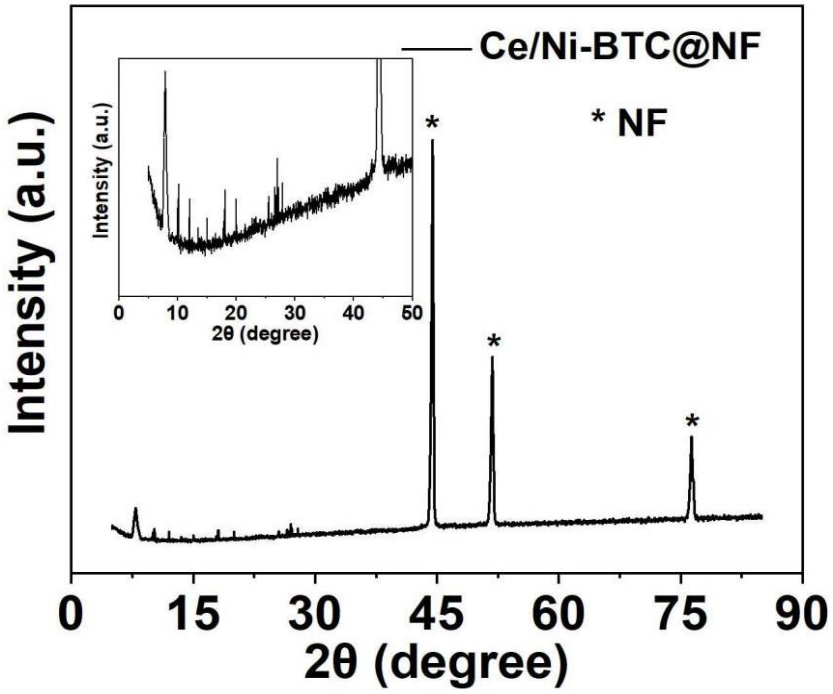

Figure 1. XRD pattern of nickel doped cerium MOF on nickel foam (Ni/Ce-BTC@NF)

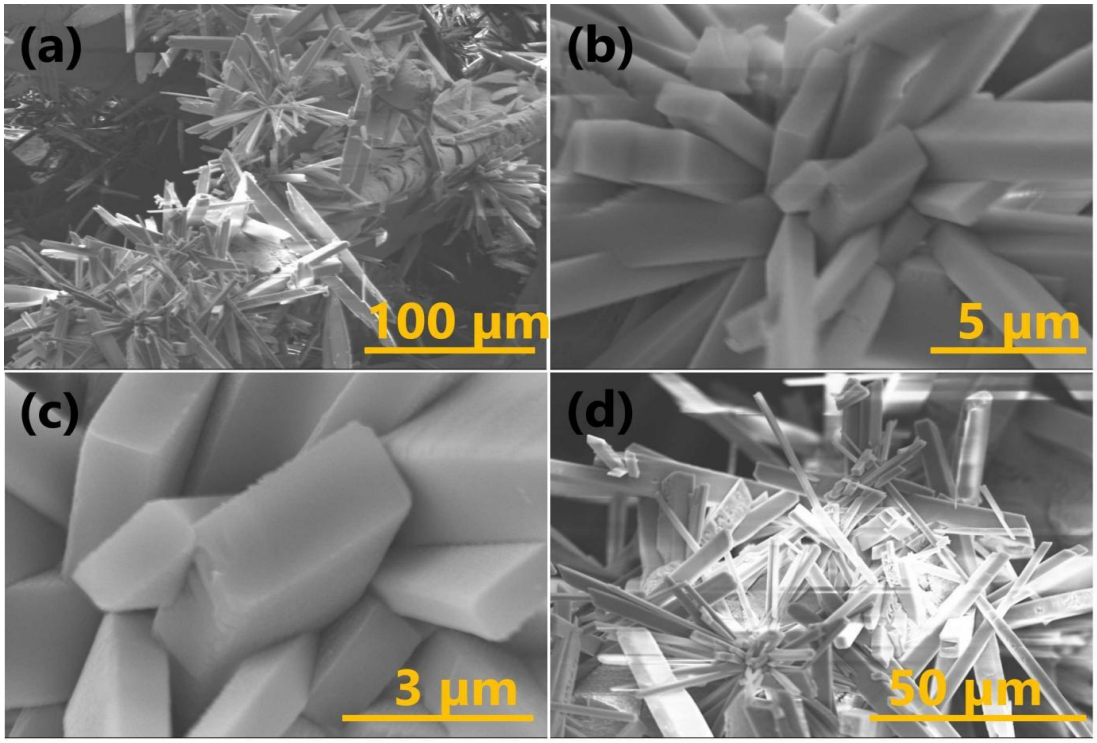

Figure 2. FESEM images of (a-c) Ni/Ce-BTC@NF, and (d) Ce-BTC@NF

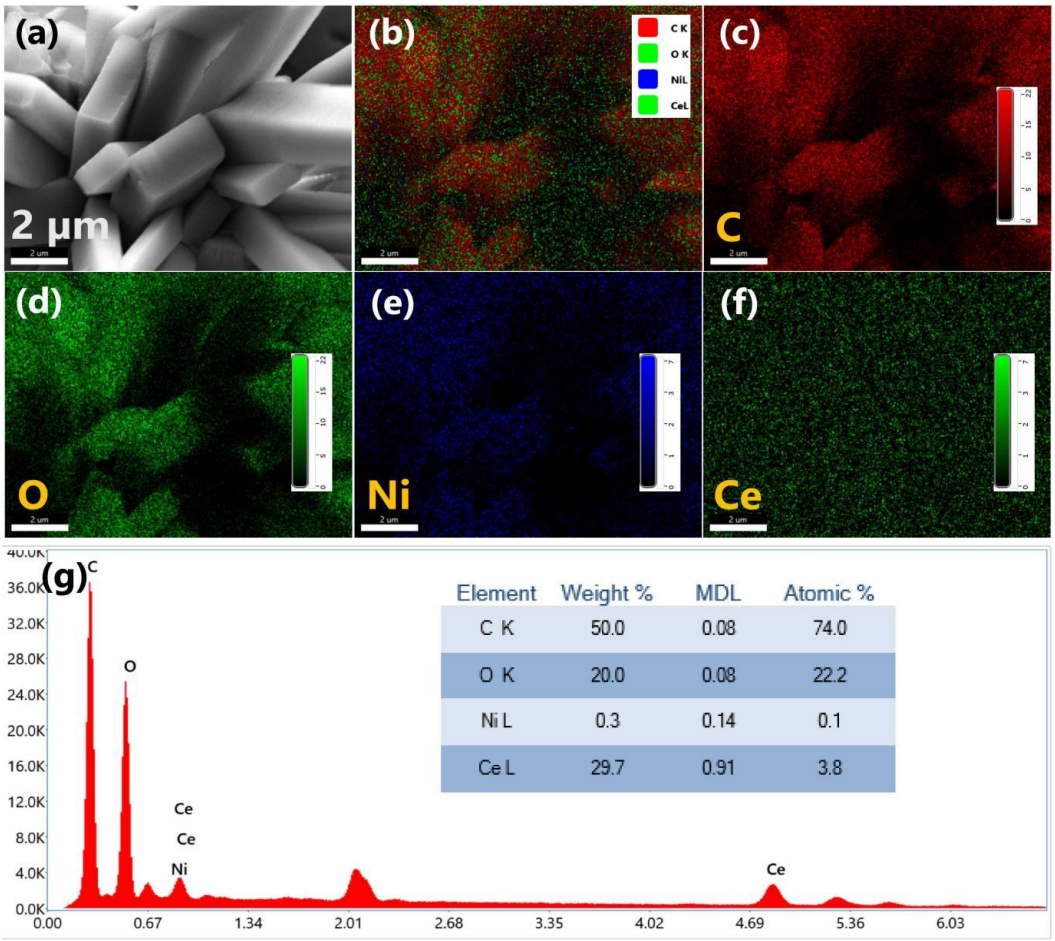

Figure 3. EDS results of Ni/Ce-BTC@NF: (a) Region selected for EDS mapping, (b) superimposition of constituent elements, and (c-f) EDS color mapping images for C, O, Ni and Ce. (g) EDS spectrum (inset: element %)

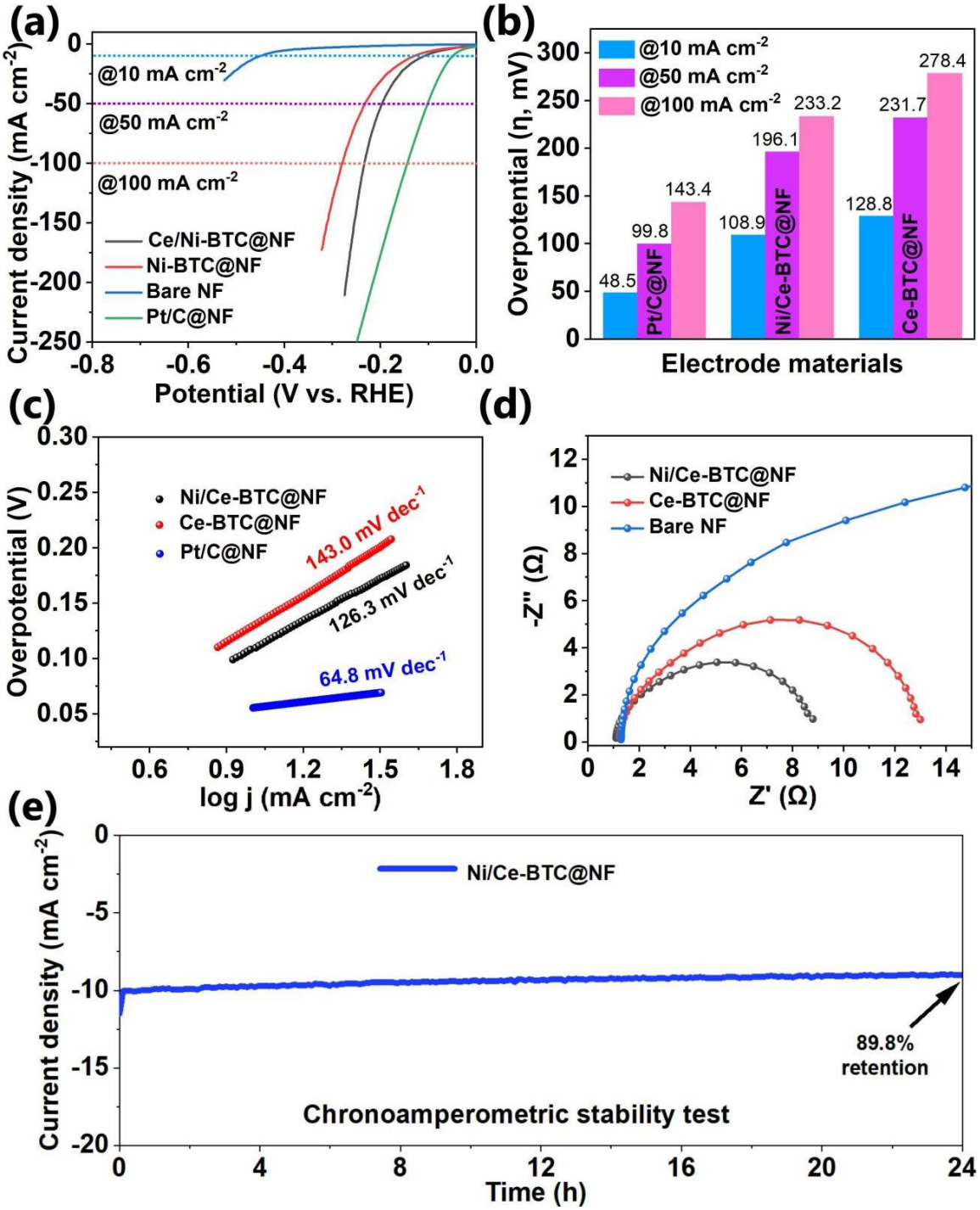

Figure 4. HER performance test results: (a) LSV curves after iR correction, (b) figure showing overpotentials of Ni/Ce-BTC@NF, Ce-BTC@NF, and Pt/C@NF at various current densities, (c) Tafel plots / slopes extracted from corresponding LSVs in Figure 4a, (d) EIS Nyquist plot, (e) chronoamperometry test result

Electrochemical performance

The electrocatalytic performance of the synthesized nanomaterials (Ce-BTC@NF and Ni/Ce-BTC@NF) toward the HER was evaluated in a three-electrode connection. Before performing each electrochemical measurement, the working electrodes were activated by 20 cyclic voltammetry (CV) cycles at 2 mV s^{-1}.

HER performance in three-electrode system

The HER action of Ce-BTC@NF and Ni/Ce-BTC@NF was assessed and compared with that of 10 wt % Pt/C and bare NF. The *iR-corrected* LSV curves taken at 2 mV s^{-1} are shown in Figure 4a. The ohmic drop caused by solution resistance was compensated using *iR* correction using the solution resistance (R_s)

values extracted from the EIS data (Nyquist plot). As shown in Figure 4b, Ni/Ce-BTC delivers the lowest overpotentials of 108.9 mV and 196.1 mV to achieve 10 mA cm^{-2} and 50 mA cm^{-2} (current densities), respectively, which are markedly lesser than those of Ce-BTC@NF (128.8 and 231.7 mV). This above par performance demonstrates that Ni doping on MOFs structure helps to enhance HER activity by modulating the electronic structure, increasing the density of active sites, easing charge transfer, and optimizing H adsorption-desorption behavior. Moreover, the Tafel slopes resulting from the HER polarization curves (Fig. 4c) reveal that Ni/Ce-BTC@NF exhibits a slope of 126.3 mV dec^{-1}, which is substantially lower than that of Ce-BTC@NF (143.0 mV dec^{-1}). The charge-transfer resistance and solution resistance of the catalysts were further evaluated by analyzing the EIS Nyquist plots (Fig. 4d). A smaller semicircular arc generally indicates faster charge-transfer processes and enhanced electronic conductivity at the electrode-electrolyte interface. Among all catalysts, Ni/Ce-BTC@NF exhibits the smallest semicircle radius, confirming its superior electron-transfer ability and more efficient HER kinetics.

The long-term durability of Ni/Ce-BTC@NF was evaluated by chronoamperometry (CA) measurements at 10 mA cm^{-2} (Fig. 4e), showing only a marginal loss in current over 24 h of continuous operation, confirming its excellent structural and electrochemical stability. The enhanced HER activity can be attributed to nickel doped electronic modulation at the Ce-MOFs structure, which accelerates both H adsorption and desorption, facilitating efficient hydrogen evolution.

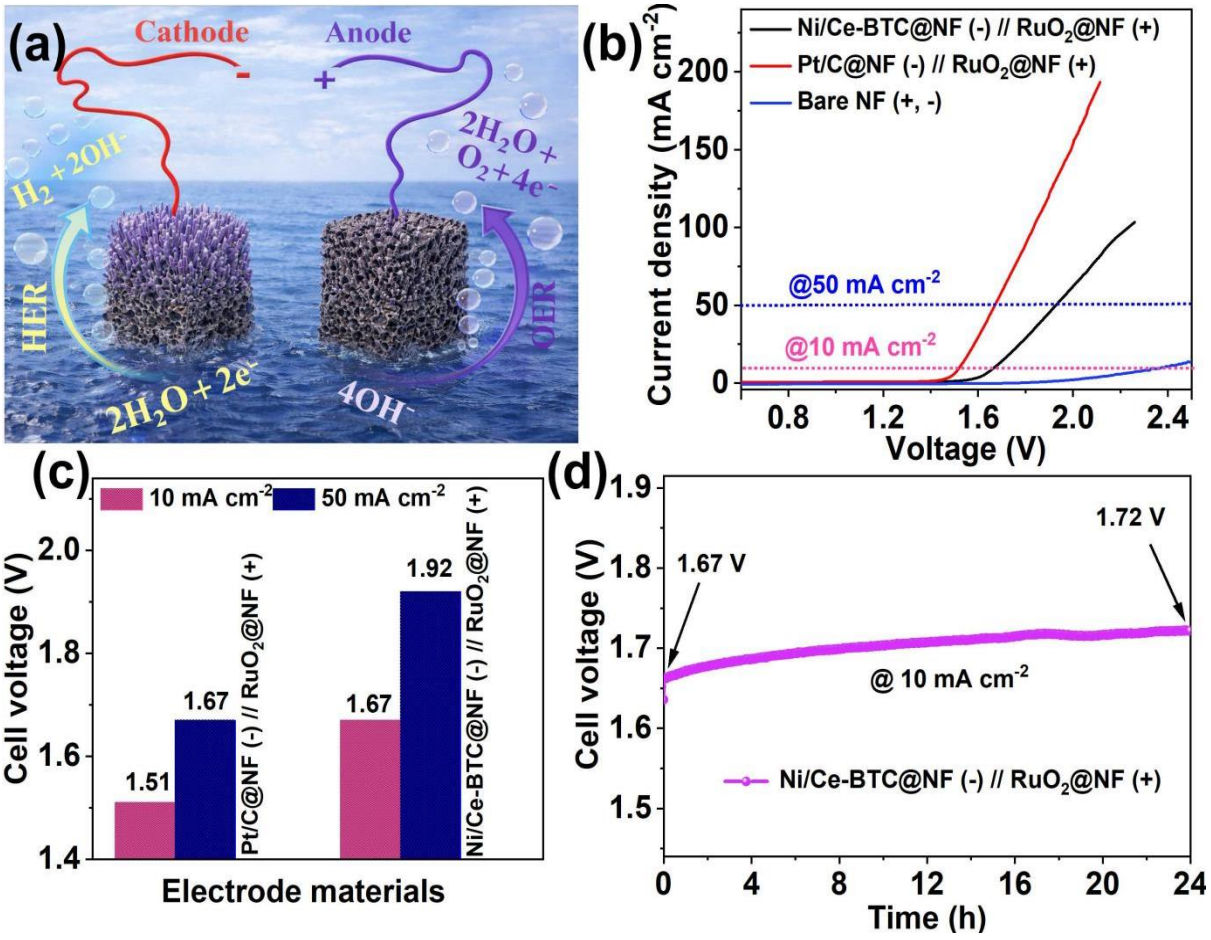

Figure 5. Electrolysis cell results: (a) Schematic illustration showing the application of Ni/Ce-BTC@NF (-) // RuO_2@NF (+) for overall water splitting, (b) polarizations curves of electrolysis cells ((Ni/Ce-BTC@NF (-) // RuO_2@NF (+), Pt/C@NF (-) // RuO_2@NF (+) and bare NF (+, -)) at scan rate of 2 mV s^{-1}, (c) cell voltages of devices at 10 mA cm^{-2} and 50 mA cm^{-2}, and (d) chronopotentiometry stability test result of device at 10 mA cm^{-2} for >24 h

Overall water-splitting performance in two-electrode system

The as-prepared Ni/Ce-BTC@NF was used as a cathode (1 × 1 cm^2), and benchmark RuO_2@NF with identical mass loading was employed as an anode (1 × 1 cm^2) for the fabrication of an electrolytic cell. Figure 5a shows the diagrammatic depiction of water electrolysis in a two-electrode arrangement and the reactions associated with HER and OER. A complete benchmark cell (Pt/C@NF (-) // RuO_2@NF (+)) and bare NF (+, -) were also assembled and tested for comparative analysis. The LSV polarization curves for each electrolysis cell are presented in Figure 5b, which show that the benchmark set outperforms the Ni/Ce-BTC@NF (-) // RuO_2@NF (+), as expected. It requires cell voltages of 1.51 V and 1.67 V only to deliver 10 mA cm^{-2} and 50 mA cm^{-2} (current densities), respectively (Fig. 5c). However, Ni/Ce-BTC@NF (-) // RuO_2@NF (+) also shows a moderate performance by requiring cell voltages of 1.67 V and 1.92 V to achieve current densities of 10 mA cm^{-2} and 50 mA cm^{-2}, respectively. This shows that Ni/Ce-BTC@NF have good performance considering its low cost. Furthermore, the bare NF cell has insignificant performance for overall water splitting as expected, indicating that the nanomaterials adhered on the NF have crucial role in the electrocatalytic process. Furthermore, the durability of the device ((Ni/Ce-BTC@NF (-) // RuO_2@NF (+)) was tested by operating chronopotentiometry stability test at 10 mA cm^{-2} (Fig. 5d). The cell voltage increased by just 0.5 V after 24 h of continuous water splitting 10 mA cm^{-2}, indicating high stability and structural integrity of the material. This work establishes Ni/Ce-BTC@NF as a promising catalyst, which can be further optimized to achieve enhanced performance.

CONCLUSION

In conclusion, we have effectively designed a nickel-doped cerium MOF (Ni/Ce-BTC) that is directly grown on 3D nickel foam as a self-supported, binder-free electrocatalyst for effective HER in alkaline environments. Ni is added to the Ce-BTC framework to create more active sites and induce electrical modulation while maintaining the intrinsic shape. The resulting hierarchical structure, which resembles a 3D nanopillar, greatly increases surface area, makes electrolyte penetration easier, and promotes dynamics of gas release. According to electrochemical studies, Ni/Ce-BTC@NF performs better in HER than pure Ce-BTC@NF, offering low overpotentials, good Tafel kinetics, lower charge-transfer resistance, and outstanding long-term durability. The improved catalytic activity is mainly accredited to the synergistic effect between Ni and Ce, which optimizes hydrogen adsorption free energy and accelerates reaction kinetics through enhanced electronic conductivity and charge redistribution. This study demonstrates how cation doping and structural engineering can effectively overcome intrinsic conductivity constraints in MOFs. The suggested approach provides insightful information for the logical development of next-generation, inexpensive, and highly effective electrocatalysts to produce hydrogen in a sustainable manner.

ACKNOWLEDGMENTS

The authors would like to acknowledge Amrit Campus, Department of Chemistry, Kathmandu, Nepal for laboratory facility, and Jeonbuk National University, Jeonju, Jeollabukdo, Republic of Korea, for material characterizations.

AUTHORS CONTRIBUTION

Conceptualization: IP; Methodology: IP; Validation: IP; Investigation: IP, PPD, BD; Data analysis: IP, PN, KRC, MN, TRA, MRK, PCL; Writing-original draft: PN; Writing-review & editing: IP; Supervision: TRA; Funding acquisition: None

FUNDING

None

ORCIDs

Ishwor Pathak:
https://orcid.org/0000-0002-8129-405X
Pujan Nepal:
https://orcid.org/0009-0007-5422-3591
Keshav Raj Chapagain:
https://orcid.org/0009-0003-0002-335X
Mani Ram Kandel:
https://orcid.org/0000-0001-5435-4566
Prakash Chandra Lohani:
https://orcid.org/0000-0001-6397-9891
Purna Prasad Dhakal:
https://orcid.org/0000-0002-3538-8004
Bipeen Dahal:
https://orcid.org/0000-0002-8269-993X
Tirtha Raj Acharya:
https://orcid.org/0000-0002-9528-280X

CONFLICT OF INTEREST

The authors declare that there are no conflicts of interest regarding the publication of this article.

DATA AVAILABILITY STATEMENT

Data can be made available upon reasonable request.

SUPPLEMENTARY INFORMATION

None

REFERENCES

Acharya, D., Chhetri, K., Pathak, I., Muthurasu, A., Mangal Bhattarai, R., Kim, T., Raj Rosyara, Y., Woo Lee, D., Hoon Ko, T., & Yong Kim, H. (2024). Multiphase lattice engineering of bimetallic phosphide-embedded tungsten-based phosphide/oxide nanorods on carbon cloth: A synergistic and stable electrocatalyst for overall water splitting. *Chemical Engineering Journal, 499*, 155832. https://doi.org/10.1016/j.cej.2024.155832

Acharya, D., Pathak, I., Muthurasu, A., Bhattarai, R. M., Kim, T., Ko, T. H., Saidin, S., Chhetri, K., & Kim, H. Y. (2023). *In situ* transmogrification of nanoarchitectured Fe-MOFs decorated porous carbon nanofibers into efficient positrode for asymmetric supercapacitor application. *Journal of Energy Storage, 63*, 106992. https://doi.org/10.1016/j.est.2023.106992

Alkhaldi, R. S., Gondal, M. A., Mohamed, M. J. S., Almessiere, M. A., Baykal, A., Caliskan, S., & Slimani, Y. (2024). Chestnut-like molybdenum-doped nickel cobaltite spinel oxide nanoparticles grown on Ni foam as the electrocatalyst for the hydrogen evolution reaction. *ACS Applied Nano Materials, 7*(3), 2867–2878. https://doi.org/10.1021/acsanm.3c05156

Amin, B. G., Swesi, A. T., Masud, J., & Nath, M. (2017). $CoNi_2Se_4$ as an efficient bifunctional electrocatalyst for overall water splitting. *Chemical Communications, 53*(39), 5412–5415. https://doi.org/10.1039/c7cc01489a

Amorim, I., Xu, J., Zhang, N., Xiong, D., Thalluri, S. M., Thomas, R., Sousa, J. P. S., Araújo, A., Li, H., & Liu, L. (2020). Bi-metallic cobalt-nickel phosphide nanowires for electrocatalysis of the oxygen and hydrogen evolution reactions. *Catalysis Today, 358*, 196–202. https://doi.org/10.1016/j.cattod.2019.05.037

Anantharaj, S., Karthick, K., Murugan, P., & Kundu, S. (2020). V^{3+} Incorporated beta-$Co(OH)_2$: A robust and efficient electrocatalyst for water oxidation. *Inorganic Chemistry, 59*(1), 730–740. https://doi.org/10.1021/acs.inorgchem.9b02977

Aryal, S., Shrestha, K. R., Shrestha, T., Oli, H. B., Pathak, I., Shrestha, R. L., & Bhattarai, D. P. (2025). Activated carbon from Prunus persica seed stones as a negatrode material for high-performance supercapacitors. *Journal of Molecular Structure, 1323*, 140810. https://doi.org/10.1016/j.molstruc.2024.140810

Chhetri, K., Acharya, D., Pawale, R. S., Kong, K.-H., Pathak, I., Rosyara, Y. R., Bhattarai, R. M., Lohani, P. C., Kim, T., Kim, N. H., Lee, J. H., Kim, B.-S., Hereijgers, J., Chung, C.-H., Cho, H., Ko, T. H., & Kim, H. Y. (2026). Hemispherical mesoporous hollow carbon nanobowls as a separator-cum-cathode material for enhanced sulfur redox kinetics and polysulfides regulation in Lithium-sulfur batteries. *Composites Part B: Engineering, 310*, 113159. https://doi.org/10.1016/j.compositesb.2025.113159

Chhetri, K., Muthurasu, A., Dahal, B., Kim, T., Mukhiya, T., Chae, S. H., Ko, T. H., Choi, Y. C., & Kim, H. Y. (2022). Engineering the abundant heterointerfaces of integrated bimetallic sulfide-coupled 2D MOF-derived mesoporous CoS_2 nanoarray hybrids for electrocatalytic water splitting. *Materials Today Nano, 17*, 100146. https://doi.org/10.1016/j.mtnano.2021.100146

Chhetri, K., Pathak, I., Acharya, D., Rosyara, Y. R., Bhattrai, R. M., Kong, K.-H., Kim, B.-S., Kim, T., Ko, T. H., & Kim, H. Y. (2025). Uniquely nanofibrillated hollow carbon nanofibers with decoration of 2D MOF-derived CoMo sulfides: An efficient cathode material for Lithium sulfur batteries. *Journal of Energy Storage, 136*, 118459. https://doi.org/10.1016/j.est.2025.118459

Dong, T., Zhang, X., Wang, P., Chen, H.-S., & Yang, P. (2020). Formation of Ni-doped MoS_2 nanosheets on N-doped carbon nanotubes towards superior hydrogen evolution. *Electrochimica Acta, 338*, 135885. https://doi.org/10.1016/j.electacta.2020.135885

Dong, T., Zhang, ., Wang, P., Chen, H.-S., & Yang, P. (2020). Formation of Ni-doped MoS_2 nanosheets on N-doped carbon nanotubes towards superior hydrogen evolution. *Electrochimica Acta, 338*. https://doi.org/10.1016/j.electacta.2020.135885

Gu, J. X., Chen, H., Ren, Y., Gu, Z. G., Li, G., Xu, W. J., Yang, X. Y., Wen, J. X., Wu, J. T., & Jin, H. G. (2022). A novel cerium(IV)-based metal-organic framework for CO_2 chemical fixation and photocatalytic overall water splitting. *ChemSusChem, 15*(1), e202102368. https://doi.org/10.1002/cssc.202102368

Gu, J. X., Zhao, P. C., Lin, W., Deng, J., Chao, Z. S., & Jin, H. G. (2024). Cerium(III)-MOF as a photocatalyst for hydrogen evolution from water splitting. *Applied Organometallic Chemistry, 38*(9), e7616. https://doi.org/10.1002/aoc.7616

Hu, Z., Wang, Y., & Zhao, D. (2021). The chemistry and applications of hafnium and cerium(iv) metal-organic frameworks. *Chemical Society Reviews, 50*(7), 4629–4683. https://doi.org/10.1039/d0cs00920b

Jacobsen, J., Ienco, A., D'Amato, R., Costantino, F., & Stock, N. (2020). The chemistry of Ce-based metal-organic frameworks. *Dalton Transactions, 49*(46), 16551–16586. https://doi.org/10.1039/d0dt02813d

Jamesh, M. I., Kuang, Y., & Sun, X. (2019). Constructing earth-abundant 3D nanoarrays for efficient overall water splitting – A review. *ChemCatChem, 11*(6), 1550–1575. https://doi.org/10.1002/cctc.201801783

Janicki, R., Mondry, A., & Starynowicz, P. (2017). Carboxylates of rare earth elements. *Coordination Chemistry Reviews, 340*, 98-133. https://doi.org/10.1016/j.ccr.2016.12.001

Jin, H. G., Wang, M., Wen, J. X., Han, S. H., Hong, X. J., Cai, Y. P., Li, G., Fan, J., & Chao, Z. S. (2021). Oxygen vacancy-rich mixed-valence cerium MOF: An efficient separator coating to high-performance lithium-sulfur batteries. *ACS Applied Materials & Interfaces, 13*(3), 3899–3910. https://doi.org/10.1021/acsami.0c18899

Liu, P., Jing, P., Xu, X., Liu, B., & Zhang, J. (2021). Structural reconstruction of Ce-MOF with active sites for efficient electrocatalytic N_2 reduction. *ACS Applied Energy Materials, 4*(11), 12128–12136. https://doi.org/10.1021/acsaem.1c01656

Liu, S., Teng, Z., Liu, H., Wang, T., Wang, G., Xu, Q., Zhang, X., Jiang, M., Wang, C., Huang, W., & Pang, H. (2022). A Ce-UiO-66 metal-organic framework-based graphene-embedded photocatalyst with controllable activation for solar ammonia fertilizer production. *Angewandte Chemie International Edition, 61*(37), e202207026. https://doi.org/10.1002/anie.202207026

Lu, X. F., Xia, B. Y., Zang, S. Q., & Lou, X. W. D. (2020). Metal-organic frameworks based electrocatalysts for the oxygen reduction reaction. *Angewandte Chemie International Edition, 59*(12), 4634–4650. https://doi.org/10.1002/anie.201910309

Luo, J., Wang, X., Gu, Y., Wang, S., Li, Y., Wang, T., Liu, Y., Zhou, Y., & Zhang, J. (2023). Hierarchical sheet-like W-doped $NiCo_2O_4$ spinel synthesized by high-valence oxyanion exchange strategy for highly efficient electrocatalytic oxygen evolution reaction. *Chemical Engineering Journal, 472*, 144839. https://doi.org/10.1016/j.cej.2023.144839

Luo, R., Luo, M., Wang, Z., Liu, P., Song, S., Wang, X., & Chen, M. (2019). The atomic origin of nickel-doping-induced catalytic enhancement in MoS_2 for electrochemical hydrogen production. *Nanoscale, 11*(15), 7123–7128. https://doi.org/10.1039/C8NR10023C

Mondal, A., & Vomiero, A. (2022). 2D transition metal dichalcogenides-based electrocatalysts for hydrogen evolution reaction. *Advanced Functional Materials, 32*(52). https://doi.org/10.1002/dfm.202208994

Naik Shreyanka, S., Theerthagiri, J., Lee, S. J., Yu, Y., & Choi, M. Y. (2022). Multiscale design of 3D metal–organic frameworks (M−BTC, M: Cu, Co, Ni) via PLAL enabling bifunctional electrocatalysts for robust overall water splitting. *Chemical Engineering Journal, 446*. https://doi.org/10.1016/j.cej.2022.137045

Pandey, S., Ghimire, M., Kim, T., Jung, M., Asaithambi, S., Dong, W. J., Son, J.-W., Yun, Y. J., & Jun, Y. (2025). Synthesis of porous MXene for efficient bifunctional electrocatalysis in overall water splitting: Hydrogen and oxygen evolution reactions. *FlatChem, 50*, 100837. https://doi.org/10.1016/j.flatc.2025.100837

Pandey, S., Ghimire, M., Lee, C., Park, J., Olivar Amaya, M. I., Trần, T. T., Son, J.-W., Yun, Y. J., & Jun, Y. (2026). Recent progress on MXene-hematite nanocomposite catalyst for water-splitting applications: Synthesis strategies, synergetic performance, and future perspectives. *Fuel, 404*, 136248. https://doi.org/10.1016/j.fuel.2025.136248

Pathak, I., Acharya, D., Chhetri, K., Chandra Lohani, P., Hoon Ko, T., Muthurasu, A., Subedi, S., Kim, T., Saidin, S., & Dahal, B. (2023). $Ti_3C_2T_x$ MXene integrated hollow carbon nanofibers with polypyrrole layers for MOF-derived freestanding electrodes of flexible asymmetric supercapacitors. *Chemical Engineering Journal, 469*, 143388. https://doi.org/10.1016/j.cej.2023.143388

Pathak, I., Acharya, D., Chhetri, K., Rosyara, Y. R., Kim, T., Ko, T. H., & Kim, H. Y. (2025). Engineering a double-mof-derived $Co_{1-x}S/Co_9S_8$ interface modulated by selenium doping and platinum single atoms: an efficient bifunctional electrocatalyst for water splitting. *ACS Applied Materials & Interfaces, 17*(28), 40443–40456. https://doi.org/10.1021/acsami.5c06979

Pathak, I., Acharya, D., Chhetri, K., Rosyara, Y. R., Muthurasu, A., Kim, T., Ko, T. H., & Kim, H. Y. (2025). Coengineering of Ni-NDC derived graphitic $Ni_2P/NiSe_2$ on a $Ti_3C_2T_x$ MXene-

modified 3D self-supporting electrode: Unraveling 2D–2D multiphases for overall water electrolysis. *Composites Part B: Engineering*, *296*, 112238. https://doi.org/10.1016/j.compositesb.2025.112238

Pathak, I., Prabhakaran, S., Acharya, D., Chhetri, K., Muthurasu, A., Rosyara, Y. R., Kim, T., Ko, T. H., Kim, D. H., & Kim, H. Y. (2024). Structural and phase engineering of a hierarchical 2D–2D nickel MOF/hydroxide-derived $Ni_{0.85}Se/NiTe_2$ heterointerface for robust HER, OER, and overall water splitting. *Small*, *20*(52), 2406732. https://doi.org/https://doi.org/10.1002/smll.202406732

Rathore, D., Banerjee, A., & Pande, S. (2022). Bifunctional tungsten-doped $Ni(OH)_2$/NiOOH nanosheets for overall water splitting in an alkaline medium. *ACS Applied Nano Materials*, *5*(2), 2664–2677. https://doi.org/10.1021/acsanm.1c04359

Rosyara, Y. R., Muthurasu, A., Chhetri, K., Pathak, I., Ko, T. H., Lohani, P. C., Acharya, D., Kim, T., Lee, D., & Kim, H. Y. (2024). Highly porous metal–organic framework entrapped by cobalt telluride–manganese telluride as an efficient bifunctional electrocatalyst. *ACS Appied Materials & Interfaces*, *16*(8), 10238. https://pubs.acs.org/doi/10.1021/acsami.3c18654

Rosyara, Y. R., Pathak, I., Muthurasu, A., Acharya, D., Chhetri, K., Kim, T., Poudel, M. B., Ojha, G. P., Ko, T. H., & Kim, H. Y. (2025). Anion-modulated bifunctional electrocatalytic activity of nickel telluride/cobalt telluride mesoporous nanosheets for high-efficiency and stable overall water splitting. *Journal of Materials Chemistry A*. *13*, 41156–41169. https://doi.org/10.1039/D5TA03463A

Senthil Raja, D., Chuah, X. F., & Lu, S. Y. (2018). In situ grown bimetallic MOF-based composite as highly efficient bifunctional electrocatalyst for overall water splitting with ultrastability at high current densities. *Advanced Energy Materials*, *8*(23), 1801065. https://doi.org/10.1002/aenm.201801065

Senthil Raja, D., Lin, H.-W., & Lu, S.-Y. (2019). Synergistically well-mixed MOFs grown on nickel foam as highly efficient durable bifunctional electrocatalysts for overall water splitting at high current densities. *Nano Energy*, *57*, 1–13. https://doi.org/10.1016/j.nanoen.2018.12.018

Shetty, S., Sadiq, M. M. J., Bhat, D. K., & Hegde, A. C. (2018). Electrodeposition of Ni–Mo–rGO composite electrodes for efficient hydrogen production in an alkaline medium. *New Journal of Chemistry*, *42*(6), 4661–4669. https://doi.org/10.1039/c7nj04552b

Sirati, M. M., Hussain, D., Mahmood, K., Chughtai, A. H., Yousaf-Ur-Rehman, M., Malik, W. M. A., Alomairy, S., Ahmed, S. b., Al-Buriahi, M. S., & Ashiq, M. N. (2022). Single-step hydrothermal synthesis of amine functionalized Ce-MOF for electrochemical water splitting. *Journal of Taibah University for Science*, *16*(1), 525–534. https://doi.org/10.1080/16583655.2022.2079310

Wang, B., Liu, S., Liu, L., Song, W.-W., Zhang, Y., Wang, S.-M., & Han, Z.-B. (2021). MOF/PEDOT/HPMo-based polycomponent hierarchical hollow micro-vesicles for high performance flexible supercapacitors. *Journal of Materials Chemistry A*, *9*(5), 2948–2958. https://doi.org/10.1039/d0ta10603h

Wang, C. P., Lin, Y. X., Cui, L., Zhu, J., & Bu, X. H. (2023). 2D metal-organic frameworks as competent electrocatalysts for water splitting. *Small*, *19*(15), e2207342. https://doi.org/10.1002/smll.202207342

Wang, H., Zhang, X., Yin, F., Chu, W., & Chen, B. (2020). Coordinately unsaturated metal–organic framework as an unpyrolyzed bifunctional electrocatalyst for oxygen reduction and evolution reactions. *Journal of Materials Chemistry A*, *8*(42), 22111–22123. https://doi.org/10.1039/d0ta04331a

Wu, L., Ning, M., Xing, X., Wang, Y., Zhang, F., Gao, G., Song, S., Wang, D., Yuan, C., Yu, L., Bao, J., Chen, S., & Ren, Z. (2023). Boosting oxygen evolution reaction of (Fe,Ni)OOH via defect engineering for anion exchange membrane water electrolysis under industrial conditions. *Advanced Materials*, *35*(44), e2306097. https://doi.org/10.1002/adma.202306097

Wu, X. P., Gagliardi, L., & Truhlar, D. G. (2018). Cerium metal-organic framework for photocatalysis. *Journal of American Chemical Society*, *140*(25), 7904–7912. https://doi.org/10.1021/jacs.8b03613

Xia, H., Zhang, J., Yang, Z., Guo, S., Guo, S., & Xu, Q. (2017). 2D MOF nanoflake-assembled spherical microstructures for enhanced supercapacitor and electrocatalysis performances. *Nanomicro Letters*, *9*(4), 43. https://doi.org/10.1007/s40820-017-0144-6

Xie, L. S., Skorupskii, G., & Dinca, M. (2020). Electrically conductive metal-organic frameworks. *Chemical Reviews*, *120*(16), 8536–

8580. https://doi.org/10.1021/acs.chemrev.9b00766

Yan, J., Kong, L., Ji, Y., White, J., Li, Y., Zhang, J., An, P., Liu, S., Lee, S. T., & Ma, T. (2019). Single atom tungsten doped ultrathin alpha-$Ni(OH)_2$ for enhanced electrocatalytic water oxidation. *Nature Communications*, *10*(1), 2149. https://doi.org/10.1038/s41467-019-09845-z

Yu, Y., Zhou, J., & Sun, Z. (2020). Novel 2D transition-metal carbides: ultrahigh performance electrocatalysts for overall water splitting and oxygen reduction. *Advanced Functional Materials*, *30*(47), 200570. https://doi.org/10.1002/adfm.202000570

Zahra, R., Pervaiz, E., Yang, M., Rabi, O., Saleem, Z., Ali, M., & Farrukh, S. (2020). A review on nickel cobalt sulphide and their hybrids: Earth abundant, pH stable electro-catalyst for hydrogen evolution reaction. *International Journal of Hydrogen Energy*, *45*(46), 24518–24543. https://doi.org/10.1016/j.ijhydene.2020.06.236

Zhang, X., Hou, F., Li, H., Yang, Y., Wang, Y., Liu, N., & Yang, Y. (2018). A strawsheave-like metal organic framework Ce-BTC derivative containing high specific surface area for improving the catalytic activity of CO oxidation reaction. *Microporous and Mesoporous Materials*, *259*, 211–219. https://doi.org/https://doi.org/10.1016/j.micromeso.2017.10.019

Zhang, X., Hou, F., Yang, Y., Wang, Y., Liu, N., Chen, D., & Yang, Y. (2017). A facile synthesis for cauliflower like CeO_2 catalysts from Ce-BTC precursor and their catalytic performance for CO oxidation. *Applied Surface Science*, *423*, 771–779. https://doi.org/https://doi.org/10.1016/j.apsusc.2017.06.235

Zhou, H. C., Long, J. R., & Yaghi, O. M. (2012). Introduction to metal-organic frameworks. *Chemical Reviews*, *112*(2), 673–674. https://doi.org/10.1021/cr300014x

Zou, Z., Cai, M., Zhao, X., Huang, J., Du, J., & Xu, C. (2019). Defective metal–organic framework derivative by room-temperature exfoliation and reduction for highly efficient oxygen evolution reaction. *Journal of Materials Chemistry A*, *7*(23), 14011–14018. https://doi.org/10.1039/c9ta02349f